This article has been accepted for publication in a future issue of this journal, but has not been fully edited. Content may change prior to final publication. Citation information: DOI 10.1109/LCOMM.2018.2854587, IEEE Communications Letters

Device-Free Motion Detection via on-the-Air LTE Signals

Sanjia Xu and Yafei Tian, *Member, IEEE*

***Abstract*— Wireless signals not only carry the information of data but also encode the information of propagation environments. The motion of an object can be sensed by analyzing the variation of channel state information. Combining the function of wireless sensing and communication will further enhance the capability of smart phones. LTE signal, which is always on the air and is seamlessly covered, is a perfect external illuminator for wireless sensing. In this paper, we study the device-free moving object detection via LTE signals. We build a prototype to receive on-the-air LTE signal and extract the real-time channel response. The existence of moving object is recognized by the amplitude of the interfered multipath, and the moving speed is derived by the phase of the dynamic reflection. The detection probability and discovery region are investigated, and field experiments are conducted to validate the analyses.**

***Index Terms*— LTE, motion detection, multipath interference, prototype, wireless sensing**

I. Introduction

With the rapid development of wireless communications, the carrier frequency and signal bandwidth are increasingly higher. The radio-frequency (RF) signal can not only be modulated to transfer information, it can also be used to perceive the propagation environment. On the signal propagation path, the variations of reflection, scattering, and diffraction will affect the channel response. Through analyzing the captured channel state information (CSI), we can find moving object, by which the dynamic reflection will cause multipath interference. In the system, the moving object only reflect the signal naturally, it does not carry any specific device.

In recent years, contactless gesture recognition and motion detection have aroused great interest. In [1], the Doppler shift of the received signal is analyzed and nine body gestures can be recognized therefrom. In [2], real-time fall detection is implemented in natural living environment, through utilizing the amplitude variation and phase difference between two receive antennas. In [3] and [4], the moving human is detected through eigenvalue analysis of the CSI amplitude and phase correlation matrices. Through-the-wall detection is studied in [5] and [6]. Since the line-of-sight (LOS) signal and static reflected signal by the wall is much stronger, MIMO precoding is used in [5] to eliminate the interference. While in [6], the difference of the eigenvectors of CSI across different subcarriers are used as detection features. The interference phenomenon between the dynamic and static reflection paths is explained in [7], and the Fresnel zone is defined as the area where the dynamic reflection path changes one wavelength. By recognizing the interfered waveforms, the resolution of motion detection increases to centimeter scale. All these researches use Wi-Fi signals as external illuminators.

However, Wi-Fi signal only covers hot-spot area, and the frame is burst in time. Since the interval of two consecutive packets is random, it is hard to track the phase in between the packets. Thus in literatures, the CSIs extracted from Wi-Fi signals are assumed to have random phases. In addition, the existed works mostly focus on patter recognition, there lacks basic analysis on the relations between the detection probability, discovery range, signal strength and reflection features.

In this paper, we study the motion detection problem via LTE signals. LTE signal is seamlessly covered and the frames are continuous in time. Even when there is no user data, the physical-layer broadcast channel (PBCH) and the cell-specific reference signal (CRS) are always on the air. Using LTE signals, we can ceaselessly monitor the environment at anywhere we are interested.

The main contribution of this paper includes three aspects:

1) we study the motion detection via LTE signals and propose a method where the motion state is estimated from the amplitude variation in CSI and the moving speed is derived from the phase difference in consecutive subframes;

2) we analyze the false alarm and missing alarm rates according to the received SNR and the reflection features, and derive the discovery region correspondingly;

3) we build a prototype system through software defined radio, and conduct field experiments to validate the models, methods and analyses.

II. System Model

In wireless communication channels, except of LOS propagation, there are multipaths caused by reflection, refraction, diffraction, and scattering. When a moving object is present in the propagation environment, the signal reflected or scattered by this object will form a dynamic path and will be combined with other static paths at the receiver, as shown in Fig. 1. Denote the baseband transmit signal as $s(t)$, the baseband received signal is

$$r(t) = \sum_{l=1}^{L-1} a_l e^{-j\frac{2\pi d_l}{\lambda}} s(t - d_l/c) + a_L(t) e^{-j\frac{2\pi d_L(t)}{\lambda}} s(t - d_L(t)/c) + n(t), \quad (1)$$

Manuscript received May 21, 2018; accepted June 22, 2018. This work was supported by the National Natural Science Foundation of China under Grants 61429101 and 61371077. The associate editor coordinating the review of this letter and approving it for publication was M. Oner. *(Corresponding author: Yafei Tian.)*

The authors are with the School of Electronics and Information Engineering, Beihang University, Beijing 100191, P. R. China (e-mail: xusanjia@buaa.edu.cn; ytian@buaa.edu.cn).

This article has been accepted for publication in a future issue of this journal, but has not been fully edited. Content may change prior to final publication. Citation information: DOI 10.1109/LCOMM.2018.2854587, IEEE Communications Letters

where the first $L-1$ paths are static paths including the LOS propagation, and the last path is dynamic path. The amplitude, phase and propagation delay of the l-th path are respectively a_l, $2\pi d_l/\lambda$, and d_l/c, where d_l is the propagation distance, λ is the carrier wavelength, and c is the light speed. The noise $n(t)$ is assumed to be additive white Gaussian with zero mean and variance σ_n^2.

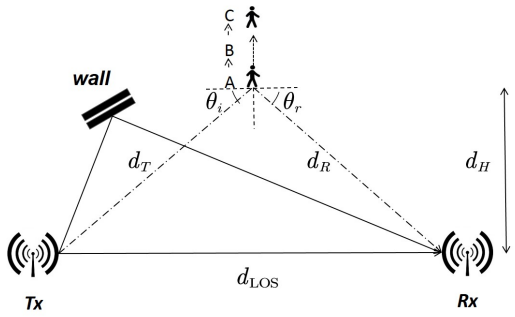

Fig. 1. Typical scenario of multipath propagation.

We only consider one moving object in this paper. This is a typical scenario in small cell or indoor environment, where usually few objects simultaneously move around the receiver. For the signal coming from a macro-cell base station (BS), although there might be many moving objects outside, their reflections will be too weak to penetrate the wall. The scenario that includes multiple moving objects will be studied in future works.

For LTE signal, we can use CRS to do channel estimation. In each subframe that with 1 ms duration, there are four OFDM symbols that contains CRS, and for 20 MHz bandwidth configuration, in each symbol there are 200 subcarriers occupied by CRS. According to (1), the channel response can be separated into static part and dynamic part, i.e.,

$$\begin{aligned} H(f,t) &= H_s(f) + H_d(f,t) + n(f,t) \\ &= H_s(f) + a_L(t)e^{-j2\pi\frac{d_L(t)}{\lambda}} + n(f,t), \end{aligned} \tag{2}$$

where H_s stands for the static part and H_d stands for the dynamic part, f denotes the baseband frequency. The channel response is represented in frequency domain, and it can be transformed to time domain as well. In frequency-flat channel, we can drop the variable f from (2) since the multiple reflection paths are inseparable.

The amplitude of the reflection path $a_L(t)$ depends on the large-scale path loss and the reflective features of the moving object. If the surface of the object is large and smooth relative to the wavelength, and the positions of Tx, Rx and the moving object agree with the reflection law, the specular reflection effect will be dominant in the received power [8], i.e.,

$$P_R\,(\mathrm{dBm}) = P_T + 20\log\frac{\Gamma\lambda}{4\pi\,(d_T+d_R)}, \tag{3}$$

where P_T denotes transmit power, and Γ is the reflective coefficient that depends on the incident angle θ_i and the relative permittivity of the material ϵ_r. From (3), we can see that in this situation the large-scale path loss depends on the sum of d_T and d_R.

Otherwise, the scattering effect is dominant. The received power will be determined by the radar cross section (RCS) of the object [8], i.e.,

$$P_R\,(\mathrm{dBm}) = P_T + 20\log\frac{\lambda}{d_T d_R} + RCS - 30\log(4\pi), \tag{4}$$

where RCS is in units of dB·m^2 and can be approximated by the surface area of the scattering object. Note that in this situation the large-scale path loss depends on the product of d_T and d_R.

In both cases, $a_L(t)$ can be calculated as

$$a_L(t) = 10^{\frac{P_R - P_T}{20}}. \tag{5}$$

III. Motion Detection Method and Analysis

A. Motion Detection Method

We will use channel estimation results $H(f,t)$ to do motion detection. Since the oscillators in transmitter and receiver are not synchronized, there is frequency-offset and phase noise in the raw CSIs. The frequency-offset estimation and compensation are implemented along with the frame synchronization. Then a phase tracking loop is applied on the strongest path to remove the phase noise. Actually, the dynamic reflection path might also be superimposed on the strongest static path and cause phase ripples. We must carefully design the phase-locked loop (PLL) to eliminate the impact of phase noise and keep the ripples caused by the moving object.

In small cell or indoor environments, the multipath delay spread is usually less than 1 μs. It is better to transform $H(f,t)$ to time-domain $h(\tau,t)$, so that the SNR of the channel estimation can be improved. For typical 20 MHz bandwidth configuration, in time domain the separable multipath delay is 50 ns and the corresponding difference of propagation distances is 15 m. That means, with high probability the dynamic path is combined in the first several delay bins.

For brevity, consider the dynamic path is in the the first delay bin, we drop the variable τ from $h(\tau,t)$, i.e.,

$$h(t) = h_s + h_d(t) + z(t), \tag{6}$$

where $z(t)$ has variance σ_z^2. When N subcarriers are occupied by CRS, $\sigma_z^2 = \sigma_n^2/N$.

We can separate the dynamic path from the superimposed static paths by using a low pass filter $F_{\mathrm{LP}}[\cdot]$, i.e.,

$$\hat{h}_s(t) = F_{\mathrm{LP}}\left[h(t)\right], \tag{7}$$

$$\hat{h}_d(t) = h(t) - \hat{h}_s(t). \tag{8}$$

The normalized standard variation of $\hat{h}_d(t)$ is calculated as the decision statistic,

$$\nu = \sqrt{\frac{1}{T}\sum_{t=t_0}^{t_0+T}|\hat{h}_d(t)|^2}\Big/|\hat{h}_s(t_0)|, \tag{9}$$

where T is the observation window. The statistic ν is a metric of amplitude fluctuation. When it is larger than a threshold ρ, we can recognize there exist moving object.

Then we can extract the phase $\phi(t) = \angle\hat{h}_d(t)$ to decide the motion orientation and speed. When $\phi(t)$ is increasing, the

This article has been accepted for publication in a future issue of this journal, but has not been fully edited. Content may change prior to final publication. Citation information: DOI 10.1109/LCOMM.2018.2854587, IEEE Communications Letters

target is moving close to the Tx-Rx LoS link, and when $\phi(t)$ is decreasing, the target is moving away. The moving speed depends on the slop of phase variation, i.e., $d\phi(t)/dt$, and the geometry relationship with the transmitter and receiver. If we want to know accurate position of the target and the absolute moving speed, we need more observations from multiple Tx-Rx pairs.

Occasionally, if the target is moving along the ellipse of the Fresnel zone, the phase of the dynamic reflection path is fixed, and there is no amplitude variation in the CSI. However, this case is rarely appeared in applications such as intruder detection, where the target is moving from outside to inside the surveillance zone. Furthermore, if we have multiple Tx-Rx pairs, they can be complementary to avoid this failure mode.

B. Detection Probability

We use false alarm rate and missing alarm rate to measure the detection performance. When there is no moving target, channel estimation errors might cause ν exceeding the threshold, which is called false alarm. On the contrast, when the moving target is indeed present, but ν has not trigger the threshold, which is called missing alarm.

The detection threshold is determined by a constant false alarm rate (CFAR). When the channel is static, the estimation $\hat{h}_d(t)$ only comprises complex Gaussian noise. Thus the statistic $\sum_{t=t_0}^{t_0+T} |\hat{h}_d(t)|^2$ is a chi-square distribution with degrees of freedom $2T$. Suppose $\hat{h}_s(t_0)$ is equal to h_s, the cumulative distribution function (CDF) of ν can be easily obtained by numerical calculations. Given the false alarm rate p_{FA}, the detection threshold ρ can be determined by

$$\Pr(\nu > \rho) = \Pr\left(\sum_{t=t_0}^{t_0+T} |z(t)|^2 > T|h_s|^2\rho^2\right) = p_{\text{FA}}, \quad (10)$$

where $\rho|h_s|/\sigma_z$ is a fixed value given p_{FA} and T.

When the channel is dynamic, $\hat{h}_d(t)$ comprises $h_d(t)$ and noise. Since $|h_d(t)| = a_L(t)$, and it is almost invariant in a observation window, the statistic $\sum_{t=t_0}^{t_0+T} |\hat{h}_d(t)|^2$ can be approximated by a non-central chi-square distribution. The missing alarm rate p_{MA} is thus

$$\Pr(\nu < \rho) = \Pr\left(\sum_{t=t_0}^{t_0+T} |a_L e^{j\phi(t)} + z(t)|^2 < T|h_s|^2\rho^2\right). \quad (11)$$

The normalized mean value a_L/σ_z can be derived from p_{MA} and $\rho|h_s|/\sigma_z$.

Fig. 2 shows the values of a_L/σ_z and $\rho|h_s|/\sigma_z$ when $p_{\text{FA}} = p_{\text{MA}}$ and $T = 100$. Actually, $|h_s|^2/\sigma_z^2$ stands for the SNR of static channels, which is N times higher than the SNR of the received signal $|h_s|^2/\sigma_n^2$. The value a_L^2/σ_z^2 stands for the SNR of the dynamic reflection path.

C. Discovery Region

Given the required detection performance p_{FA} and p_{MA}, we can determine the required a_L according to a_L/σ_z and $|h_s|/\sigma_z$. Define the relative reflective strength

$$\gamma = \frac{a_L}{|h_s|} = \frac{a_L/\sigma_z}{|h_s|/\sigma_z}. \quad (12)$$

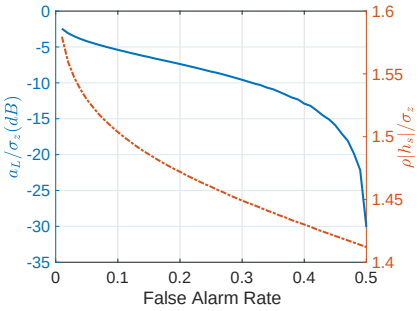

Fig. 2. The calculated values of a_L/σ_z and $\rho|h_s|/\sigma_z$.

The required channel gain of the dynamic path is $a_L = \gamma|h_s|$. The channel gain of static paths is

$$|h_s| = \frac{\lambda}{4\pi d_{\text{LOS}}}, \quad (13)$$

when there is only LOS propagation. Otherwise, $|h_s|$ should be a measured result.

Then the discovery region can be derived from equations (3)-(5). Assuming that (13) is satisfied, for the reflective model, the discovery region is defined by an ellipse, i.e.,

$$d_T + d_R \le \frac{\Gamma\lambda}{4\pi a_L} = \frac{\Gamma}{\gamma} d_{\text{LOS}}. \quad (14)$$

For the scattering model, the discovery region is defined by a Cassini oval, i.e.,

$$d_T d_R \le \frac{\lambda}{a_L} \cdot 10^{\frac{RCS - 30\log(4\pi)}{20}} = \frac{d_{\text{LOS}}}{\sqrt{4\pi\gamma}} \cdot 10^{\frac{RCS}{20}}. \quad (15)$$

IV. Experiment Results

We designed a prototype system to receive LTE signals. The RF part is implemented on AD-FMCOMMS2, which is an evaluation board of AD9361. The baseband processing is on ZedBoard, an evaluation board of Xilinx Zynq-7020. To reduce the implementation complexity and get real-time results, for each subframe of LTE signal we only extract one time of channel estimation. This is equivalent to 1 ms sampling interval to the channel response.

We use another prototype to transmit LTE signal, so that the measurement environment is under control. The transmit power is 1 mW and the carrier frequency is 2.3 GHz. There is LOS propagation between the transmitter and receiver, and their distance is set as 5 m. The measured SNR of the static channel response is 37 dB, and this corresponds to 14 dB for the SNR of the received signal. A walking human is tested as the moving object, whose RCS is assumed to be 0.5 m^2, and the relative permittivity of the clothes is 5.

A snapshot of the observed channel response is shown in Fig. 3, where the person is moving back-and-forth along the perpendicular line of the Tx-Rx connection. Both the amplitude of the overall channel response and the phase of the dynamic reflection path are presented. In one second, the distance of the dynamic reflection path reduces about 3λ and then recovers again. From Fig. 3, we can see 6 periods of amplitude fluctuation, and the phase of the dynamic path first

This article has been accepted for publication in a future issue of this journal, but has not been fully edited. Content may change prior to final publication. Citation information: DOI 10.1109/LCOMM.2018.2854587, IEEE Communications Letters

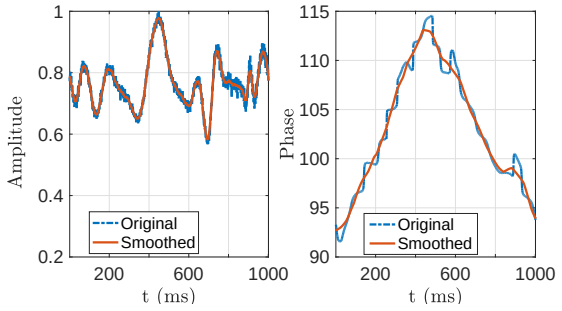

Fig. 3. A snapshot of the observed channel response in motion state.

increases 6π and then decreases 6π. These observations are consistent with the assumptions in system model.

The next experiment is to validate the reflection strength model. In Section II, we have introduced reflective model and scattering model, which have different power degradations. We still let the person moving on the perpendicular line and record the power of the dynamic reflection path. The SNRs of the dynamic reflection path are shown in Fig. 4. We can see that the measured result is more close to the scattering model.

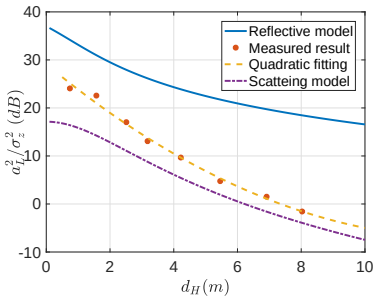

Fig. 4. The measured SNR of the dynamic reflection path.

The detection probability is tested in the same environment. The observation window is set as 100 ms, and the detection threshold is set when the false alarm rate is 10%. The missing alarm rate is measured when the person moves along the perpendicular line. We sampled 40 groups of CSI, and for each group there is 1000 decision statistics in 1 m distance interval. From Fig 5, we can see that the missing alarm rate increase dramatically when d_H exceeds 7 meters, where from Fig. 4 we know that the SNR of the dynamic path a_L^2/σ_z^2 starts below 0 dB.

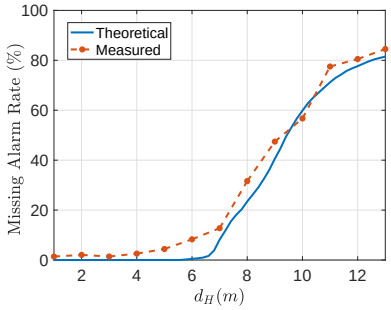

Fig. 5. Missing alarm rates at different locations.

On the contrast of moving on the perpendicular line, we test the discovery region that let the object moving in various directions. The target will be discovered when $a_L^2/\sigma_z^2 \geq 0$ dB. The boundary of the discovery region is drawn in Fig. 6, where the theoretical values are calculated by (15). The larger region is caused by the walking human and the smaller region is caused by the moving hand. The lines and markers represent the theoretical and measured results, respectively. We can see that the discovery region changes with different RCSs and the Cassini oval has different shape with different parameters.

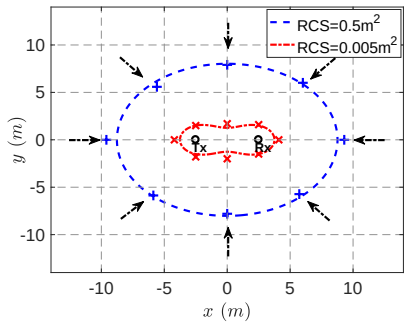

Fig. 6. Discovery regions with different RCSs.

We also tested the system by receiving on-the air LTE signals, either from small-cell BS or from macro-cell BS. No matter with or without LOS propagation, the properties that we have shown above are the same. If the received SNR is higher or d_{LOS} is larger, the discovery region can be expanded correspondingly.

V. Conclusion

In this paper, we studied the motion detection via LTE signals. We first formulate the channel model depending on the reflective features of moving objects. Then we propose a detection method using amplitude fluctuation and phase variation of the extracted CSI. The false alarm and missing alarm rates are analyzed, and the discovery region is derived. The models, methods and analyses are validated by field experiments on a prototype system. It was shown that motion detection with LTE signals is feasible and promising.

References

[1] Q. Pu, S. Gupta, S. Gollakota, and S. Patel, "Whole-home gesture recognition using wireless signals," in *ACM MOBICOM 2013*, pp. 27–38.

[2] H. Wang, D. Zhang, Y. Wang, and et al., "RT-Fall: A real-time and contactless fall detection system with commodity WiFi devices," *IEEE Trans. Mobile Comput.*, vol. 16, no. 2, pp. 511–526, Feb. 2017.

[3] C. Wu, Z. Yang, Z. Zhou, and et al., "Non-invasive detection of moving and stationary human with WiFi," *IEEE J. Sel. Areas Commun.*, vol. 33, no. 11, pp. 2329–2342, Nov. 2015.

[4] K. Qian, C. Wu, Z. Yang, and et al., "Enabling contactless detection of moving humans with dynamic speeds using CSI," *ACM Trans. Embed. Comput. Syst.*, vol. 17, no. 2, pp. 52:1–18, Jan. 2018.

[5] F. Adib and D. Katabi, "See through walls with Wi-Fi," in *ACM SIGCOMM 2013*, vol. 43, no. 4, pp. 75–86.

[6] H. Zhu, F. Xiao, L. Sun, and et al., "R-TTWD: Robust device-free through-the-wall detection of moving human with WiFi," *IEEE J. Sel. Areas Commun.*, vol. 35, no. 5, pp. 1090–1103, May 2017.

[7] D. Zhang, H. Wang, and D. Wu, "Toward centimeter-scale human activity sensing with Wi-Fi signals," *Computer*, vol. 50, no. 1, pp. 48–57, Jan. 2017.

[8] T. S. Rappaport, *Wireless Communications: Principles and Practice*. Prentice Hall PTR, 1996.